

## Amorphization and Molecular Dissociation of SnI<sub>4</sub> at High Pressure

N. Hamaya, K. Sato, and K. Usui-Watanabe

*Department of Physics, Ochanomizu University, Bunkyo, Tokyo 112, Japan*

K. Fuchizaki

*Department of Physics, Kyushu University 33, Fukuoka 812, Japan*

Y. Fujii

*Neutron Facility, ISSP, The University of Tokyo, Tokai, Ibaraki 319-11, Japan*

Y. Ohishi\*

*Tsukuba Research Laboratory, Sumitomo Chemical Co. Ltd., Tsukuba, Ibaraki 302, Japan*

(Received 3 October 1996; revised manuscript received 12 September 1997)

Synchrotron x-ray diffraction study establishes a novel structure sequence in SnI<sub>4</sub> at high pressures to 153 GPa. A new crystalline phase responsible for the metallization is observed above 7.2 GPa. The pressure-amorphized SnI<sub>4</sub> emerging above 15 GPa crystallizes at 61 GPa into another new structure having an apparent fcc lattice with a nearest-neighbor distance as short as 3.00 Å. This provides evidence for the occurrence of molecular dissociation. Atomic arrangement in the nonmolecular phase and structural properties of the amorphous state are discussed. [S0031-9007(97)04593-6]

PACS numbers: 61.50.Ks, 62.50.+p, 64.70.Kb

The compression of molecular crystals can produce drastic changes in their bonding properties and electronic structures. The insulator-metal transition in rare gas solid Xe provides a clear example [1]. In diatomic molecular crystal I<sub>2</sub>, the gradual insulator-metal transition proceeds at first [2]. Further compression forces its molecular bonding to break up and to stabilize a monatomic crystal form [3]. This phenomenon, called molecular dissociation, was also found in Br<sub>2</sub> [4]. The bonding property changes in a different way in pentatomic molecular crystals SnI<sub>4</sub> [2,5] and GeI<sub>4</sub> [6]; they transform simultaneously to a metallic and amorphous phase.

At atmospheric pressure, SnI<sub>4</sub> crystallizes into a cubic lattice with space group  $Pa\bar{3}$  and with eight molecules packing loosely in the unit cell ( $a = 12.273$  Å at room temperature) [7]. The gradual pressure-induced metallization of SnI<sub>4</sub> above 7 GPa (in the revised pressure scale) was first reported by Riggelman and Drickamer [2] in their electric resistivity measurements. The x-ray diffraction study by Fujii *et al.* [5] revealed that a halo pattern gradually developed between 10 and 20 GPa and persisted to at least 33 GPa. This observation was taken as evidence for the pressure-induced amorphization of SnI<sub>4</sub>. Since then, metallic amorphous SnI<sub>4</sub> has been studied extensively. A Raman study to 25 GPa by Sugai [8] demonstrated that the (SnI<sub>4</sub>)<sub>2</sub> dimer formed in the amorphous state. From their Mössbauer study, Pasternak and Taylor [9] suggested the formation of randomly oriented poly-tin-tetraiodide conducting chains. An x-ray-absorption fine structure (XAFS) study by Wang and Ingalls [10] led them to propose a model structure consisting of distorted SnI<sub>4</sub> molecules linked with smaller tetrahedral units of iodine atoms. Although those three models are different, all studies indicate

the presence of the SnI<sub>4</sub> molecule below 25 GPa. None of the pentatomic molecular crystals have so far manifested themselves in an atomic crystalline form resulting from molecular dissociation under pressure.

Those rich results then raise a number of questions on structural evolution of SnI<sub>4</sub> at high pressure: How does the ordered arrangement of molecules vary into the disordered one? To what extent does the amorphous SnI<sub>4</sub> exist? If it changes, what is a resultant structure? Do SnI<sub>4</sub> molecules still remain or already break up in the new structure? Furthermore, are there any structural changes in the amorphous SnI<sub>4</sub> as observed in the amorphous ice at high pressure [11]? Those questions motivated us to perform the present synchrotron x-ray diffraction study of SnI<sub>4</sub> at high pressures up to 153 GPa. In this Letter, we report, for the first time, evidence for molecular dissociation in a pentatomic molecular crystal. We document a new crystalline-crystalline phase transition prior to the amorphization and a structural change in the amorphous state.

Polycrystalline SnI<sub>4</sub> of 99.9% purity, supplied by Kojundo Chemical Co., was further purified by sublimation at 105 °C in vacuum. Obtained crystals were ground, placed in a cavity drilled in a T-301 stainless steel gasket with ruby chips, and loaded in a modified Mao-Bell-type diamond anvil cell in an argon atmosphere. Five separate runs were carried out at room temperature. A mixture of normal pentane and isopentane supersaturated with SnI<sub>4</sub> was used as a pressure medium in one run up to 9.3 GPa. This run was dedicated to the precise determination of atomic positions in the  $Pa\bar{3}$  phase. No pressure medium was loaded in the other four runs, in one of which powdered gold as a pressure standard in a megabar pressure range was added to the sample. We employed the ruby fluorescence technique

for pressure calibration below 70 GPa. Above 70 GPa, the pressure was determined from the lattice constant of gold with the aid of the equation of state given by Anderson *et al.* [12]. Synchrotron x-ray diffraction measurements were carried out at BL6B and BL18C of the Photon Factory at KEK. Wavelength was tuned with a Si(111) double-crystal monochromator to 0.6888 Å in three runs, to 0.5166 Å in one run, and to 0.6199 Å in the other. To achieve high angular resolution and reliable intensity collection over a wide dynamic range, an imaging plate detector was used. The details of the present high pressure diffractometry has been described elsewhere [13].

Previous studies suggested that the  $Pa\bar{3}$  cubic structure (crystal phase I designated as CP-I) directly transformed to the amorphous state. If this is the case, one may expect anomalous atomic movements in CP-I as the structural disordering develops with increasing pressure. Figures 1(a) and 1(b) show typical diffraction patterns for CP-I. Although the pressure transmitting fluid solidified at 6.2 GPa, diffraction peaks remained very sharp at 6.6 GPa. As seen in Fig. 1(b), the result of the Rietveld refinement [14] is fairly good. Sets of five independent positional parameters were obtained at several pressures below 6.6 GPa. Calculating bond lengths from them, we observed that the average Sn-I distance decreased only slightly from  $2.65 \pm 0.02$  Å at 1 atm to  $2.63 \pm 0.04$  Å at 6.6 GPa, being consistent with the XAFS result [10].

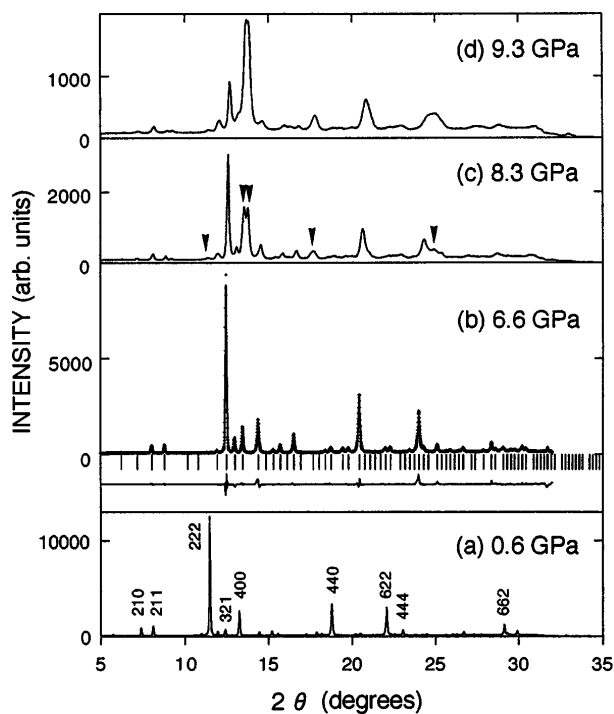


FIG. 1. Sequence of x-ray diffraction patterns with increasing pressure showing a phase transition at 7.2 GPa. Indices of major reflections from the  $Pa\bar{3}$  structure are given in (a) and the Rietveld refinement plot for the same structure at 6.6 GPa is shown in (b). Two phases coexist in (c) and (d) and major new peaks are denoted by arrows.

The average intramolecular I-I distance also changes a little from  $4.33 \pm 0.03$  Å at 1 atm to  $4.32 \pm 0.01$  Å at 6.6 GPa. The covalent bonded  $\text{SnI}_4$  molecule is rigid and does not deform in CP-I. On the other hand, the intermolecular I-I distances ranging from 4.198 to 4.516 Å at 1 atm decrease dramatically but monotonically with increasing pressure and are in the range of 3.664 to 3.898 Å at 6.6 GPa. This large contraction can be understood as a result of the weakness of the van der Waals bonding between molecules. Consequently, below 6.6 GPa we find no indication of either distortion of the molecule nor symmetry breaking of CP-I, and hence no precursor of the structural disordering.

To our surprise, several new, sharp diffraction peaks appeared at 7.2 GPa prior to the amorphization. Figures 1(c) and 1(d) show, respectively, diffraction patterns measured at 8.3 and 9.3 GPa, where the new crystalline phase, designated as CP-II, coexists with CP-I. When the pressure was reduced from 9.3 GPa, the reverse transition took place at 5.4 GPa, indicating that the CP-I–CP-II phase transition is of first order. According to the previous results [2,5], the drastic decrease in electric resistivity begins at 7 GPa. This strongly suggests that the structural change from CP-I to CP-II is the insulator-metal phase transition. Since previous studies [8–10] indicate the presence of the  $\text{SnI}_4$  molecule below 25 GPa, CP-II is expected to be a metallic molecular crystalline phase.

Figure 2 shows some selected diffraction patterns measured above 10 GPa. The CP-I–CP-II transition was observed between 7.6 and 9.7 GPa under a nonhydrostatic condition. Diffraction peaks in Figs. 2(a) and 2(b) were slightly broadened by nonhydrostaticity of the pressure and by overlapping of the CP-I and CP-II reflections. We observed that much broader scattering appeared above 15 GPa at  $2\theta \sim 14^\circ$ , suggesting formation of an “x-ray amorphous” phase. The progress of the disordering is so gradual that the strongest reflection of CP-II still remained to at least 21 GPa [Fig. 2(c)]. Diffraction patterns typical of those in amorphous materials were observed between 24 and 55 GPa [Figs. 2(d) and 2(e)].

At 61 GPa, the amorphous state transformed into a crystalline phase CP-III showing a simple diffraction pattern [Fig. 2(f)]. As indexed in this figure, observed reflections can be explained by the fcc lattice with a lattice constant of  $4.248 \pm 0.002$  Å. The nearest-neighbor distance is calculated to be  $3.003 \pm 0.001$  Å. A particularly interesting fact is that this value is the same as that of  $3.00 \pm 0.02$  Å measured in  $\text{I}_2$  having the monatomic, fcc structure at 64 GPa [15]. Further compression of  $\text{SnI}_4$  demonstrated that CP-III was stable to 153 GPa and its  $P$ - $V$  relation curve coincided with that reported for the fcc iodine [16] with precision better than  $\Delta V/V \sim 0.025$ . Those facts immediately suggest an idea of the phase separation of  $\text{SnI}_4$  into pure iodine and pure tin. Tin has the bcc structure over a pressure range of 45–120 GPa [17]. Taking account of the stoichiometry of  $\text{SnI}_4$ , we estimate that the intensity of the 110 reflection of the bcc tin is  $\sim \frac{1}{3}$

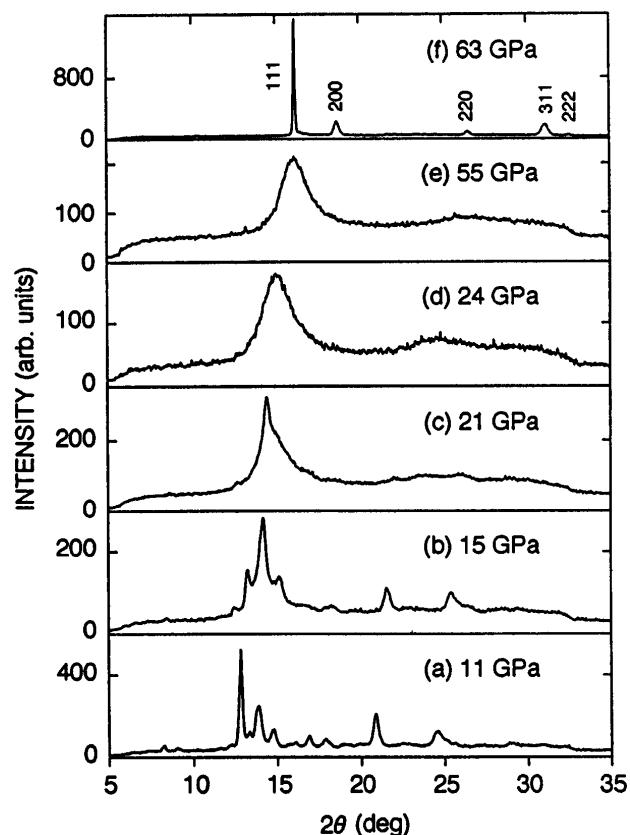


FIG. 2. Selected x-ray diffraction patterns measured upon compression. Crystalline phase II coexists with crystalline phase I in (a), becomes dominant in (b), and is partially disordered in (c). The amorphous state, (d) and (e), transforms at 61 GPa to crystalline phase III showing reflections that can be indexed with the fcc lattice (f).

times that of the 111 reflection of the fcc iodine. Such a strong reflection should be detected feasibly with the present instrumental capability; nevertheless, we observed no extra reflections from the sample above 61 GPa in three different runs. This fact eliminates the possibility of the presence of the bcc tin in  $\text{SnI}_4$ . Furthermore, this gives negative evidence for the formation of any crystalline phases of  $\text{SnI}_2$  which may be produced when molecular dissociation  $\text{SnI}_4 \rightarrow \text{SnI}_2 + \text{I}_2$  occurs.

There are three structure models that can account for the observed diffraction pattern in Fig. 2(f). The first is a partially disordered structure, in which four iodine atoms form a regular fcc unit cell, while a tin atom randomly occupies one of the tetrahedral interstitial sites. This model, however, seems unlikely in terms of the compression behavior because this structure has a density of  $13.5 \text{ g/cm}^3$  at 61 GPa much higher than that of the fcc iodine,  $10.9 \text{ g/cm}^3$ , and is expected to be less compressible than the fcc iodine. The second model is a fully disordered structure; both tin and iodine atoms are randomly placed at the fcc lattice sites. The third is a phase separation into the fcc  $\text{I}_2$  and amorphous tin or  $\text{SnI}_2$ . We were not able to distinguish those model structures in the present x-ray diffraction study. Observation of the local structure around

the tin atom is crucial to test those models and clarify the atomic arrangement in CP-III. In any case, the realization of the fcc lattice with the nearest-neighbor distance as short as  $3.00 \text{ \AA}$  provides evidence for the occurrence of molecular dissociation in  $\text{SnI}_4$ .

The pressure was then decreased from 63 GPa in one run and from 153 GPa in another. In both cases, the broadening of crystalline peaks began at 40 GPa and the halo pattern reappeared at 30 GPa. As seen in Fig. 3, the amorphous state remained down to 1.8 GPa. At 0.4 GPa, it crystallizes into the original molecular-crystalline structure even after the molecular dissociation. Careful examination of the measured diffraction patterns shows that there is a discontinuous change in halo peak position between 3.6 and 1.8 GPa. This anomaly is consistent with the Raman observation that two  $A_1$  breathing modes merge into a single peak at 2 GPa on decreasing pressure [8]. Those facts suggest the occurrence of structural change associated with the dimer to monomer transformation in the amorphous state. The pressure-induced amorphous-amorphous transformation has also been observed in ice [11] and  $\text{GeO}_2$  [18].

Reproducing the low-pressure amorphous state at 2.3 GPa on decompression from 27 GPa in the other run, we compressed it again up to 36 GPa. No crystallization was observed throughout this second cycle. What we measured are two discrete jumps of the halo peak position at 5.8 and 13 GPa, as seen in Fig. 4. Thus, we can distinguish three amorphous states (AS); AS-I at  $P < 6 \text{ GPa}$ , AS-II at 6–13 GPa, and AS-III at  $P > 13 \text{ GPa}$ . Note the correspondence between those transformation pressures in the amorphous state and the pressures where the crystalline phases undergo phase transitions. It is clear that the stability of AS-I is strongly correlated with CP-I and AS-II with CP-II. Similar behavior is also known in  $\text{GeO}_2$  [18], in which the coordination number of the Ge atom in the amorphous and the crystalline phases

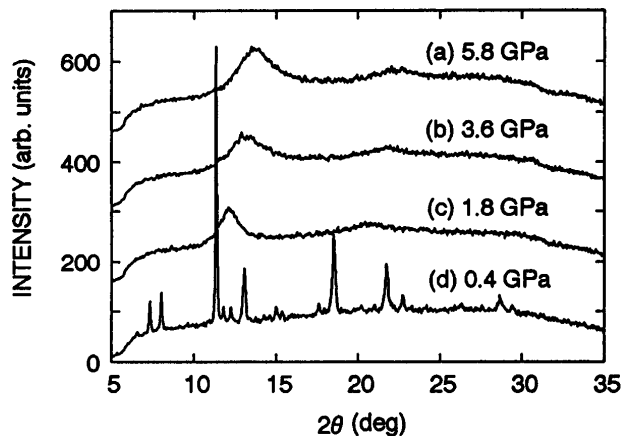


FIG. 3. Sequence of x-ray diffraction patterns with decreasing pressure. The high-pressure amorphous state, (a) and (b), transforms to the low-pressure amorphous state (c). The original molecular-crystalline phase reappears at 0.4 GPa (d), coexistent with the remnants of the amorphous phase.

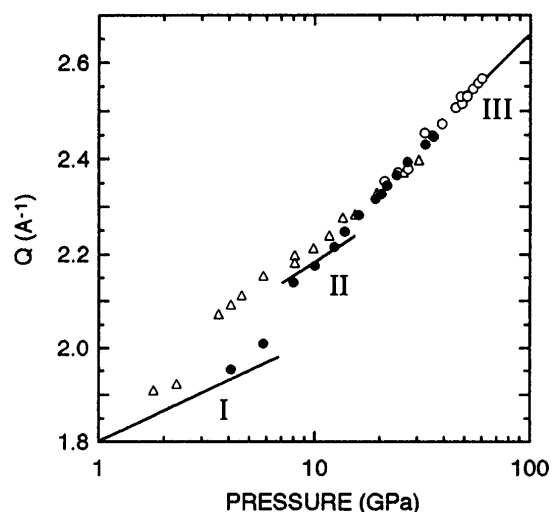


FIG. 4. Wave number  $Q$  of the first halo peak plotted as a function of pressure. Open circles and open triangles denote  $Q$  measured in the first compression and decompression, respectively. Solid circles denote  $Q$  measured in the second compression. Solid line indicates the wave number of the strongest reflection of the crystalline phase denoted as I, II, and III.  $Q$  values were determined with precision better than  $\pm 0.02 \text{ \AA}^{-1}$ . The halo peak position changes discontinuously at 2.3 GPa on the first decompression and at 5.8 and 13 GPa on the second compression, suggesting the occurrence of structural changes in the amorphous state.

changes at the same pressure. Another correlation can be found in the variation of peak position with pressure. As observed in Fig. 4, in AS-I and AS-II the amorphous halo peak is positioned very near the strongest reflection of the corresponding crystalline structure measured in the first cycle. From those observations, we infer that the amorphous  $\text{SnI}_4$  consists of microcrystals of the corresponding crystalline phase and that their translational, long-range order is not high enough to probe with the x-ray wavelength used in this study. AS-III exhibits the identical compression behavior to the initially observed amorphous state, whose first halo apparently turns into the 111 reflection of CP-III. This implies that AS-III has closer structural relation to CP-III than CP-II. This observation may awaken a new interest in amorphous structure near the recrystallization pressure.

In summary, we have established the detailed process of structural evolution of  $\text{SnI}_4$  under pressure. Determination of the crystal structure of the metallic molecular phase is important in clarifying whether or not this is an intermediate phase prior to the amorphization, as found in  $\alpha$ -quartz [19]. Recently, the superconducting transition was observed at  $T_c = 1.96 \text{ K}$  in the atomic crystalline phase of  $\text{SnI}_4$  at 64 GPa [20]. This is much higher than  $T_c = 0.7 \text{ K}$  measured for the fcc iodine at 60 GPa [21]. To explain the difference in  $T_c$ , further experimental and theoretical studies are required.

We thank T. Yagi, T. Kikegawa, and O. Shimonura for their technical advice. N.H. acknowledges the support of

this work by Ito Science Foundation and by the Grant-in-Aid for Science Research from the Ministry of Education, Science and Culture. This work was carried out under the proposal (No. 94G336) approved by the PF-PAC.

\*Present address: JASRI, SPring-8, Kamigori, Hyogo 678-12, Japan.

- [1] R. Reichlin, K.E. Brister, A.K. McMahan, M. Ross, S. Martin, Y.K. Vohra, and A.L. Ruoff, *Phys. Rev. Lett.* **62**, 669 (1989).
- [2] M. Riggelman and H.G. Drickamer, *J. Chem. Phys.* **38**, 2721 (1963).
- [3] K. Takemura, S. Minomura, O. Shimonura, and Y. Fujii, *Phys. Rev. Lett.* **45**, 1881 (1980).
- [4] Y. Fujii, K. Hase, Y. Ohishi, H. Fujihisa, N. Hamaya, K. Takemura, O. Shimomura, K. Kikegawa, Y. Amemiya, and T. Matsushita, *Phys. Rev. Lett.* **63**, 536 (1989).
- [5] Y. Fujii, M. Kowaka, and A. Onodera, *J. Phys. C* **18**, 789 (1985).
- [6] M.P. Pasternak, R.D. Taylor, M.B. Kruger, R. Jeanloz, J.P. Itie, and A. Polian, *Phys. Rev. Lett.* **72**, 2773 (1994).
- [7] R.G. Dickinson, *J. Am. Chem. Soc.* **45**, 958 (1923); F. Meller and I. Fankuchen, *Acta Crystallogr.* **8**, 343 (1955).
- [8] S. Sugai, *J. Phys. C* **18**, 799 (1985).
- [9] M.P. Pasternak and R.D. Taylor, *Phys. Rev. B* **37**, 8130 (1988).
- [10] F. Wang and R. Ingalls, *High Pressure Science and Technology*, edited by W.A. Trzeciakowski (World Scientific, Singapore, 1996), p. 289.
- [11] O. Mishima, L.D. Calvert, and E. Whalley, *Nature (London)* **310**, 393 (1984).
- [12] O.L. Anderson, D.G. Isaak, and S. Yamamoto, *J. Appl. Phys.* **65**, 1534 (1989).
- [13] O. Shimomura, K. Takemura, H. Fujihisa, Y. Fujii, Y. Ohishi, T. Kikegawa, Y. Amemiya, and T. Matsushita, *Rev. Sci. Instrum.* **63**, 967 (1992).
- [14] F. Izumi, *The Rietveld Analysis*, edited by R.A. Young (Oxford University, New York, 1993).
- [15] Y. Fujii, K. Hase, N. Hamaya, Y. Ohishi, A. Onodera, O. Shimomura, and K. Takemura, *Phys. Rev. Lett.* **58**, 796 (1987).
- [16] R. Reichlin, A.K. McMahan, M. Ross, S. Martin, J. Hu, R. J. Hemley, H.K. Mao, and Y. Wu, *Phys. Rev. B* **49**, 3725 (1994).
- [17] S. Desgreniers, Y.K. Vohra, and A.L. Ruoff, *Phys. Rev. B* **39**, 10359 (1989).
- [18] J.P. Itie, A. Polian, G. Calas, J. Petiau, A. Fontain, and H. Tolentino, *Phys. Rev. Lett.* **63**, 398 (1989).
- [19] K.J. Kingma, R.J. Hemley, H.K. Mao, and D.R. Veblen, *Phys. Rev. Lett.* **70**, 3927 (1993).
- [20] N. Takeshita, S. Kometani, K. Shimizu, K. Amaya, N. Hamaya, and S. Endo, *J. Phys. Soc. Jpn.* **65**, 3400 (1996).
- [21] K. Shimizu, N. Tamitani, N. Takeshita, M. Ishizuka, K. Amaya, and S. Endo, *J. Phys. Soc. Jpn.* **61**, 3853 (1992).